

Bootstrap tomography of high-precision pulses for quantum control

V. V. Dobrovitski,¹ G. de Lange,² D. Ristè,² and R. Hanson²

¹*Ames Laboratory US DOE, Iowa State University, Ames IA 50011, USA*

²*Kavli Institute of Nanoscience Delft, Delft University of Technology,
P.O. Box 5046, 2600 GA Delft, The Netherlands*

(Dated: October 29, 2018)

Long-time dynamical decoupling and quantum control of qubits require high-precision control pulses. Full characterization (quantum tomography) of imperfect pulses presents a bootstrap problem: tomography requires initial states of a qubit which can not be prepared without imperfect pulses. We present a protocol for pulse error analysis, specifically tailored for a wide range of the single solid-state electron spins. Using a single electron spin of a nitrogen-vacancy (NV) center in diamond, we experimentally verify the correctness of the protocol, and demonstrate its usefulness for quantum control tasks.

PACS numbers: 76.30.-v, 03.65.Wj, 76.30.Mi, 76.60.-k

Coherent manipulation of single and few electron spins has recently been achieved in several solid-state systems such as quantum dots and diamond defect centers. Such systems are promising candidates for quantum information processing [1, 2], precise metrology [3] and ultra-sensitive magnetometry [4]. They also present an excellent testbed for studying the fundamental problems of quantum dynamics of open systems [5–7]. High-speed manipulation of the system’s quantum state can be achieved by using microwave or optical pulses [8–10], which must be fine-tuned to provide a high degree of fidelity. For example, sequences of quantum control pulses can be used to extend the coherence time via dynamical decoupling [11–14, 16]. For long sequences, even small errors in the pulses will destroy the coherence that one attempts to preserve [14, 15] and may even lead to artificial saturation [17, 18]. Therefore, precise characterization of errors is essential for successful implementation of complex quantum control protocols. With known errors, composite pulses and/or special pulse sequences can be chosen to mitigate the problem.

Complete information on the action of a pulse can in principle be gained with quantum process tomography (QPT) [19]. However, QPT of an imperfect pulse requires preparation and measurement of a complete set of reference states, whereas in many solid-state qubit systems (e.g. quantum dots, diamond defect centers, superconducting circuits) only one state can be prepared reliably (without the imperfect pulses), and only one observable can be directly measured. All other states can be prepared only with the imperfect pulses themselves, and therefore have errors [20]. This presents a bootstrap problem: the reference states contain the very same errors that we want to determine.

The problem of pulse error analysis has been studied extensively in the areas of NMR and ESR [21–24]. However, single electron spins in solid-state settings present new opportunities and challenges, and call for new approaches tailored at the specific demands of these sys-

tems. The driving pulse field can be tightly confined in the vicinity of the target spin. The resulting strong, nanosecond-timescale pulses enable fast spin manipulation, but the standard pulse error analysis [21–24] used in NMR becomes inapplicable. At strong driving, the spin dynamics changes noticeably [10]. The non-secular terms in the rotating frame can become important. The ac-Stark and Bloch-Siegert shifts can significantly detune the pulse frequency from resonance [10] and tilt the rotation axis towards the z -axis. Also, the pulse edges constitute a much larger fraction of the short pulse, and the driving field at the edges varies much faster and stronger than in typical NMR pulses. The resulting errors [10] (e.g. tilting of the rotation axis) can go beyond the standard treatment [25], and can not always be removed by symmetrizing the pulse shape.

Also, typical NMR systems have long coherence times that exceed the pulse width by orders of magnitude. The standard tune-up protocols [21–24] exploit this advantage, and use sequences with tens or hundreds of pulses to achieve outstanding precision in pulse parameters. But single solid-state electron spins are dephased faster, on a timescale T_2^* of microseconds down to tens of nanoseconds [5]. After only tens of pulses the signal becomes a complex mixture of pulse errors and decoherence [17, 18]. To ensure a reliable measurement of the errors, the protocol for single electron spins must be short, a few pulses at most.

Here, we present a systematic approach to pulse characterization for single solid-state electron spins, which is usable at shorter coherence times and much stronger driving power compared to traditional NMR systems. The proposed protocol contains four series of measurements, each having only 1–3 pulses, thus minimizing the effect of decoherence. The measured signal quantifying the pulse errors grows linearly with the errors to ensure a good accuracy for small errors. Also, the signal is zero for zero errors for good relative accuracy. The protocol determines all pulse errors: the rotation angle and all

three components of the rotation axis [25]. We experimentally demonstrate the protocol on a single spin of a nitrogen-vacancy (NV) defect center in diamond. By deliberately introducing known pulse errors, we verify the accuracy and self-consistency of the protocol, and use it to significantly increase the fidelity of QPT.

Our goal is to determine the parameters of four pulses, π_X , π_Y , $\pi/2_X$, and $\pi/2_Y$ applied to a two-level quantum system (π_X denotes a rotation by an angle π around the x -axis in the rotating frame; other notations are analogous). These pulses allow implementation of universal decoupling XY sequences [11, 12], full tomography of the density matrix, and universal single-qubit gates [19]. We assume that the pulse errors are reasonably small, and consider only the first-order terms in these quantities (since we want the signal to grow proportionally to errors). We also assume that the pulse width t_p is small in comparison with the dephasing time T_2^* ; in this case the impact of decoherence is of second order, $(t_p/T_2^*)^2$, and is negligible for short sequences [25]. Under this assumption the evolution of a spin during the pulse can be described a unitary rotation. For example, for $S = 1/2$, the evolution (in the rotating frame) during an imperfect π_X pulse is given by

$$U_X = e^{-i(\vec{n}\vec{\sigma})(\pi+2\phi)/2} \approx -\phi - i(\sigma_x + \epsilon_y\sigma_y + \epsilon_z\sigma_z), \quad (1)$$

where $\sigma_{x,y,z}$ are the Pauli matrices, the rotation angle error is 2ϕ and the rotation axis \vec{n} has small components $n_y = \epsilon_y$ and $n_z = \epsilon_z$. Similarly, a $\pi/2_X$ pulse U'_X has the rotation angle error $2\phi'$, and the small rotation axis components ϵ'_y and ϵ'_z along y and z , respectively. Note that in general two $\pi/2$ pulses do not yield the same evolution as one π pulse due to errors introduced by the pulse edges. Analogous parameters for y -pulses will be denoted as 2χ , v_x , and v_z (angle and axis errors for π_Y), and $2\chi'$, v'_x , and v'_z (angle and axis errors for $\pi/2_Y$).

The bootstrap protocol shares ideas with the standard QPT, and with the NMR tune-up sequences. Before each measurement, the spin is in the state $|\uparrow\rangle$, and the measured signal is $\langle\psi|\sigma_z|\psi\rangle$, where $|\psi\rangle$ is the wavefunction after the pulse. An imperfect pulse U_j can be represented as a product $U_j = U_j^{(0)}V_j \approx U_j^{(0)}(\mathbf{1} - iK_j)$, where $U_j^{(0)}$ is a corresponding ideal rotation and the Hermitian operator K_j is proportional to small pulse errors. Applying two pulses U_1 and U_2 in succession, we obtain up to linear order in K_j

$$U_{21} = U_2U_1 \approx U_2^{(0)}U_1^{(0)} - iU_2^{(0)}K_1 - iK_2U_1^{(0)}, \quad (2)$$

and the terms $U_2^{(0)}K_1$ and $K_2U_1^{(0)}$ contain different matrix elements of the operators K_1 and K_2 . E.g., if U_1 and U_2 are the (imperfect) $\pi/2_Y$ and $\pi/2_X$ rotations, the signal detected after this sequence, $S_{21} = \text{Tr}(\sigma_z U_{21} |\uparrow\rangle\langle\uparrow| U_{21}^\dagger)$, contains a linear combination of the matrix elements $\langle\uparrow|K_1|Y\rangle$ and $\langle\uparrow|K_2|X\rangle$ (where $|Y\rangle = |\uparrow\rangle + i|\downarrow\rangle$)

TABLE I: Summary of the bootstrap protocol: pulse sequences (read from right to left) and the resulting signals expressed in terms of the error parameters. Blocks of sequences are separated by horizontal lines.

Sequence	Signal
$\pi/2_X$	$-2\phi'$
$\pi/2_Y$	$-2\chi'$
$\pi/2_X - \pi_X$	$2(\phi + \phi')$
$\pi/2_Y - \pi_Y$	$2(\chi + \chi')$
$\pi_Y - \pi/2_X$	$-2v_z + 2\phi'$
$\pi_X - \pi/2_Y$	$2\epsilon_z + 2\chi'$
$\pi/2_Y - \pi/2_X$	$-\epsilon'_y - \epsilon'_z - v'_x - v'_z$
$\pi/2_X - \pi/2_Y$	$-\epsilon'_y + \epsilon'_z - v'_x + v'_z$
$\pi/2_X - \pi_X - \pi/2_Y$	$-\epsilon'_y + \epsilon'_z + v'_x - v'_z + 2\epsilon_y$
$\pi/2_Y - \pi_X - \pi/2_X$	$-\epsilon'_y - \epsilon'_z + v'_x + v'_z + 2\epsilon_y$
$\pi/2_X - \pi_Y - \pi/2_Y$	$\epsilon'_y - \epsilon'_z - v'_x + v'_z + 2v_x$
$\pi/2_Y - \pi_Y - \pi/2_X$	$\epsilon'_y + \epsilon'_z - v'_x - v'_z + 2v_x$

and $|X\rangle = |\uparrow\rangle + |\downarrow\rangle$). Combining different pulses, we obtain a sufficient number of such linear combinations of various matrix elements of K_j to uniquely determine all of them. A general approach to bootstrap tomography can be formulated in the language of QPT, by expanding the operation element operators [19] in terms of small errors, and various bootstrap protocols applicable to more complex systems can be designed in a similar manner. Here, we focus on a protocol for a single two-level system.

The proposed protocol is summarized in Table I. It consists of three blocks of measurement sequences. For each sequence the measured signal is given in terms of the error parameters. The first block, with two single-pulse sequences, yields the rotation angle errors for the $\pi/2$ pulses. This information is then used in the second block, consisting of four two-pulse sequences, to find the rotation angle errors and the components of the rotation axis along z for the π pulses. The third block has six multi-pulse sequences, yielding six signals that are linearly related to the remaining six pulse error parameters. This linear system is underdetermined, since the whole system of pulses is invariant under rotations around the z -axis. We may put $\epsilon'_y = 0$, taking the phase of the $\pi/2_X$ pulse as the x direction in the rotating frame. This fixes all other directions, and all errors are uniquely determined. No unphysical results, typical for experimental implementations of standard QPT [20, 27], appear in this bootstrap protocol.

We now demonstrate and verify the protocol experimentally by applying it to a single solid-state spin system. We use the spin of a single Nitrogen-Vacancy (NV) center, which is a defect in diamond composed of a substitutional nitrogen atom with an adjacent vacancy [26]. The NV center's spin can be optically initialized and read

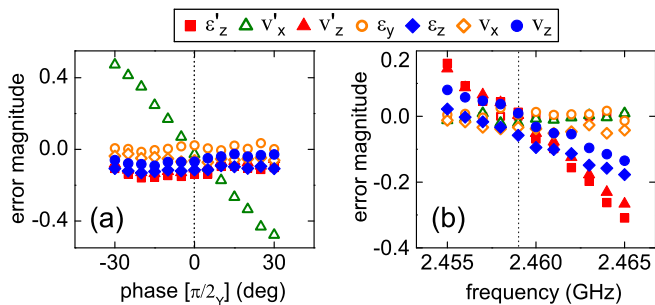


FIG. 1: (Color online) Experimental verification of the bootstrap protocol by introducing varying pulse errors. Duration of the $\pi/2$ -pulses (π -pulses) is 5 ns (9 ns). (a) Measured error parameters for different phases Φ of the $\pi/2_Y$ -pulse. The frequency of the driving field is set at 2.4605 GHz. (b) Measured error parameters for various frequencies of the driving field. Error bars everywhere are smaller than the symbol size.

out [26]. The experiments are performed in a home-built confocal microscope at room temperature. NV centers in nanocrystals are prepared on a chip with a lithographically-defined waveguide allowing fast and precise spin rotations by magnetic resonance [25].

We controllably introduce two types of pulse errors, and use the bootstrap protocol to extract their values. In the first experiment, we vary the phase Φ of the nominal $\pi/2_Y$ -pulse between -30° and 30° from its nominal value. This way, we are changing the error parameter $v'_x = \sin \Phi \approx \Phi(\text{rad})$ while leaving all other error parameters constant. Figure 1(a) shows the results from the bootstrap protocol that clearly support this expectation.

In the second experiment we detune the microwave excitation away from the qubit transition frequency, thereby varying the z -components of the rotation axis for all pulses. As shown in Fig. 1(b), the extracted error parameters v_z , v'_z , ϵ_z , and ϵ'_z strongly change (roughly linearly) with the detuning as expected, while the other error parameters stay virtually constant. If these rotation axis errors were arising only from the bulk of the pulse, they would all show the same dependence on the detuning, and all four curves would have the same slope. Instead we observe that the errors of the nominal $\pi/2$ -pulses vary about twice as much as the errors of the nominal π -pulses. This indicates that the errors originate largely from the pulse edges. Since the edges are the same for all pulses, they have a relatively larger impact on shorter pulses. The data in Fig. 1(a)-(b) demonstrate that the bootstrap protocol is indeed an efficient and reliable tool for extracting pulse errors.

Due to experimental limitations it may be impossible to cancel all errors at once. In that case, the choice of the optimal working point involves a trade-off, and precise knowledge of the pulse errors becomes particularly important. For example, when performing QPT, a set of the reference states is prepared using the pulses π_X ,

$\pi/2_X$, and $\pi/2_Y$. These states are acted upon by the process, and rotated to the readout basis before measurement [19]. The operation elements of the quantum process are expanded in the basis $E_0 = I$, $E_1 = \sigma_x$, $E_2 = \sigma_y$, and $E_3 = \sigma_z$, and the process is completely characterized by the 4×4 expansion matrix χ [19]. When systematic pulse errors are present, the prepared initial states differ from the reference states, and the read-out is also performed in the incorrect basis, yielding an incorrect matrix χ . But with pulse errors known, the raw measured data can be transformed into the correct basis prior to the standard QPT data processing [19, 20, 27].

As a demonstration, and as a check of self-consistency of the bootstrap protocol, we perform QPT while introducing the same pulse errors as in Fig. 1. We show that with the pulse errors deduced with the protocol, the QPT results can be corrected. The comparison between raw and corrected data below is designed to use no *a priori* assumptions about correctness of the bootstrap protocol.

First, we take the (imperfect) π_Y pulse as an example of a quantum process. We introduce errors in the QPT procedure by changing the phase Φ of the nominal $\pi/2_Y$ -pulse from -30° to 30° . We first determine the reference process which corresponds to $\Phi = 0$; the corresponding experimental settings and the pulse error parameters are marked in Figs. 1 and 2 by dotted lines. We perform QPT on this reference process, and the resulting reference matrix χ_0 is calculated in two ways: (i) using the raw uncorrected data, i.e. assuming that the pulses used for QPT are ideal (we denote this matrix as χ_0^i), and (ii) using the data corrected for the known pulse imperfections (the resulting matrix is χ_0^c). Next, we vary Φ , and use artificially deteriorated $\pi/2_Y$ pulses to determine the matrix χ of the quantum process. This matrix is also determined in two way, by using raw experimental data (matrix χ^r), and by correcting the data for the known pulse errors (matrix χ^c). For each value of Φ , we compare the raw-data matrices χ^r and χ_0^i on one hand, and the corrected matrices χ^c and χ_0^c on the other.

The process we are studying does not depend on the phase of the nominal $\pi/2_Y$ pulse. Thus, ideally, the matrices χ_0 and χ should be the same. To quantify the difference between χ_0 and χ , we use two distance measures. One is the process fidelity [19] $F = \text{Tr}[\chi_0 \chi]$, which depends quadratically on the pulse errors. The other measure is the Hilbert-Schmidt 2-norm $\|M\|_2 = \sqrt{\text{Tr}[MM^\dagger]}$ of the difference matrix $M = \chi - \chi_0$. This norm is linear in, and thus more sensitive to, the pulse errors [28].

In Figs. 2(a)-(b), orange squares show the values of F and $\|M\|_2$ for the corrected-data matrices χ_0^c and χ^c . The expectation that χ_0 and χ should coincide is confirmed with excellent precision. Almost independently of Φ , the fidelity remains above 99%, and $\|M\|_2$ stays small. This is not so for the raw-data matrices χ_0^i and χ^r (blue squares). The neglected phase error of the nominal $\pi/2_Y$ pulse makes the matrix χ^r inaccurate, so F and $\|M\|_2$

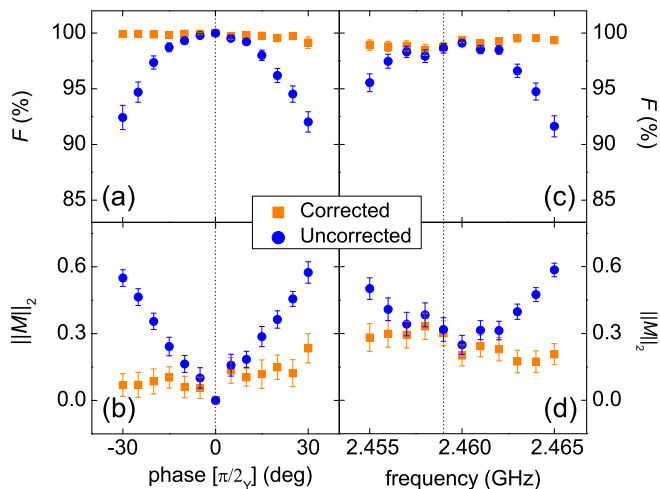


FIG. 2: (Color online) Correction of pulse errors in Quantum Process Tomography using the bootstrap protocol. (a) Fidelity (F) and (b) the 2-norm distance $\|M\|_2$ between the process measured at finite introduced $\pi/2_\gamma$ phase error and the process matrix measured at zero introduced error. The process is a π_γ -pulse with zero introduced error. (c) F and (d) $\|M\|_2$ between the measured process and the actual process (identity). All measures are calculated both for the uncorrected and for the corrected data.

depend on Φ , with fidelity dropping by 8% for $\Phi = 30^\circ$.

In a second experiment, we detune the microwave excitation frequency away from the qubit transition, introducing the errors ϵ_z , ϵ'_z , v_z , and v'_z (see Fig. 1b) into all pulses. The tomographed process is the identity process, which is independent of the pulse carrier frequency. We perform QPT on this process for the same range of detunings as in Fig. 1(b). As above, we determine the corrected and the uncorrected matrices χ^r , and χ^c , while the matrix χ_0 , describing the identity process, is independent of the pulse errors. The results are shown in Fig. 2(c)–(d). Again, the fidelities are high for the corrected data for the full range of introduced errors, while for the uncorrected data the fidelity has dropped by as much as 10%. The same behavior is seen for $\|M\|_2$. Thus, even the effects of complex pulse errors introduced by detuning the frequency can be efficiently corrected using the information from the bootstrap protocol.

Summarizing, we have developed an effective pulse error analysis protocol tailored to the specific requirements of single solid-state spins. We have experimentally implemented and verified the protocol on a single electron spin in diamond. We have shown that the distortions of the tomography results, arising due to the pulse errors, can be corrected with the knowledge obtained from the bootstrap protocol. The methods described in this paper are applicable to many systems. They may help in accurate determination of the properties of different quantum processes, a key feature for the fields of quantum information processing, quantum metrology and fundamental

studies of quantum decoherence.

We would like to thank D. G. Cory, S. Lyon, A. Tyryshkin, M. Pruski, C. Ramanathan, K. Schmidt-Rohr, and M. Laforest for very useful and enlightening discussions. Work at Ames Laboratory was supported by the Department of Energy — Basic Energy Sciences under Contract No. DE-AC02-07CH11358. We gratefully acknowledge support from FOM, NWO and the DARPA QuEST program.

-
- [1] D. Loss and D.P. DiVincenzo, *Phys. Rev. A* **57**, 120 (1998).
 - [2] L. Childress *et al.*, *Phys. Rev. Lett.* **96**, 070504 (2006).
 - [3] J. A. Jones *et al.*, *Science* **324**, 1166 (2009); P. Cappellaro *et al.*, *Phys. Rev. Lett.* **94**, 020502 (2005); J. M. Geremia, J. K. Stockton, and H. Mabuchi, *Phys. Rev. Lett.* **94**, 203002 (2005).
 - [4] J. M. Taylor *et al.*, *Nature Physics* **4**, 810 (2008); C. Degen, *Appl. Phys. Lett.* **92**, 243111 (2008); G. Balasubramanian *et al.*, *Nature* **455**, 648 (2008).
 - [5] R. Hanson and D. D. Awschalom, *Nature* **453**, 1043 (2008).
 - [6] L. Childress *et al.*, *Science* **314**, 281 (2006); R. Hanson *et al.*, *Science* **320**, 5874 (2008); D. J. Reilly *et al.*, *Phys. Rev. Lett.* **101**, 236803 (2008), C. Latta *et al.*, *Nature Physics* **5**, 758 (2009); I. T. Vink *et al.*, *Nature Physics* **5**, 764 (2009).
 - [7] C. H. Tseng *et al.*, *Phys. Rev. A* **61**, 012302 (1999); S. Lloyd, *Science* **273**, 1073 (1996).
 - [8] J. Berezovsky *et al.*, *Science* **320**, 349 (2008); D. Press *et al.*, *Nature* **456**, 218 (2008); Y. Wu *et al.*, *Phys. Rev. Lett.* **99**, 097402 (2007).
 - [9] P. Neumann *et al.*, *Science* **320**, 1326 (2008); L. Jiang *et al.*, *Science* **326**, 267 (2009).
 - [10] G. D. Fuchs *et al.*, *Science* **326**, 1520 (2009).
 - [11] L. Viola, E. Knill, and S. Lloyd, *Phys. Rev. Lett.* **82**, 2417 (1999); L. F. Santos and L. Viola, *Phys. Rev. Lett.* **97**, 150501 (2006).
 - [12] K. Khodjasteh and D. Lidar, *Phys. Rev. Lett.* **95**, 180501 (2005).
 - [13] M. J. Biercuk *et al.*, *Nature* **458**, 996 (2009).
 - [14] J. Du *et al.*, *Nature* **461**, 1265 (2009).
 - [15] H. De Raedt *et al.*, *Prog. Theor. Phys. Suppl.* **145**, 233 (2002).
 - [16] J. J. L. Morton *et al.*, *Nature Physics* **2**, 40 (2006).
 - [17] W. Zhang *et al.*, *Phys. Rev. B* **77**, 125336 (2008); W. Zhang *et al.*, *J. Phys.: Cond. Matter* **19**, 083202 (2007).
 - [18] D. Li *et al.*, *Phys. Rev. Lett.* **98**, 190401 (2007).
 - [19] M. A. Nielsen and I. L. Chuang, *Quantum Computations and Quantum Information* (Cambridge University Press, Cambridge, 2002).
 - [20] J. M. Chow *et al.*, *Phys. Rev. Lett.* **102**, 090502 (2009);
 - [21] B. C. Gerstein and C. R. Dybowski, *Transient Techniques in NMR of Solids* (Academic Press, Orlando, 1985).
 - [22] D. P. Burum, M. Linder, and R. R. Ernst, *J. Mag. Res.* **43**, 463 (1981).
 - [23] A. J. Shaka *et al.*, *J. Mag. Res.* **80**, 96 (1988).
 - [24] U. Haubenreisser and B. Schnabel, *J. Mag. Res.* **35**, 175 (1979).

- [25] See the supplementary material.
- [26] F. Jelezko and J. Wrachtrup, *J. Phys.: Cond. Matter* **16**, R1089 (2004).
- [27] M. Howard *et al.*, *New J. Phys.* **8**, 33 (2006).
- [28] The 2-norm $\|M\|_2$ is based on a quadratic function of

the elements of the χ and χ_0 matrices; hence it includes the rms of experimental noise. The fidelity F , for a fixed χ_0 , is a linear combination of the elements of χ .